2022 44th Annual International Conference of
the IEEE Engineering in Medicine & Biology Society (EMBC)
Scottish Event Campus, Glasgow, UK, July 11-15, 2022

2022 44th Annual International Conference of the IEEE Engineering in Medicine & Biology Society (EMBC) | 978-1-7281-2782-8/22/$31.00 ©2022 IEEE | DOI: 10.1109/EMBC48229.2022.9871245

Development of a Simulation Software Algorithm for High-End Mechanical Ventilators with Functionalities to attend COVID-19 Patients

Victor Ticllacuri[1,2,3,**], Sebastian Ibarra[1,2], Katherin Zumaeta[1,2,3], Estiven Torres[1,2,3], Marco Mendoza[1,2], Allan Flores[3]

***Abstract*— More than 500 millions of people were affected by the COVID-19 pandemic and in Peru there is an increasing the high numbers of cumulative cases; as well as the hospitalized people, where more than 20% require mechanical ventilation. This condition with other respiratory diseases cause patients to remain connected to a mechanical ventilator until they regain the ability to perform this vital function on their own. Some prototypes with characteristics equivalent to a high-end mechanical ventilator have been developed. And therefore, this paper presents the design and simulation of an algorithm for the pressure-controlled pulmonary ventilation mode of the mechanical ventilator. The functional design of the algorithm uses the linear multi compartment mathematical model to simulate the respiratory system. Finally the results respond adequately under multiple scenarios, including variations of the ventilator and pulmonary parameters, where the algorithm presents encouraging results in the mechanical ventilator simulation.**

***Clinical relevance*—The algorithm presented in this study will allow to have better knowledge for a treatment and eventual clinical diagnosis in health centers, especially in eventual variants and outbreaks of COVID-19.**

I. Introduction

The COVID-19 pandemic has represented a global crisis that affected more than 300 millions of people. Particularly, according to the Ministerio de Salud of Peru, there are 2.31 millions cumulative cases until 2021; and approximately the 21,92% of hospitalized people need mechanical ventilation to recover its ability to fulfill vital breathing function on their own. This virus causes acute respiratory distress syndrome and other respiratory disease that force patients to be connected to a mechanical ventilator. The use of this medical equipment becomes demanding considering that, in Peru, there were not enough high-end mechanical ventilators to meet the demand of patients and provide adequate care. Additionally, the medical devices industry is still poor in Peru, as well as the high dependence on foreign technology to satisfy health needs.

Alternatively, multiple emergency ventilators were developed as a result of collaboration between industry, academia and government; such as [1] or [2]. Therefore, the *Pontificia Universidad Católica del Perú* (PUCP) developed a prototype comparable with a high-end mechanical ventilator. However, the software for empirical contrast of this ventilator is not complete. Thus, this study aims to develop an algorithm for the modes of pulmonary ventilation considering the physiological parameters.

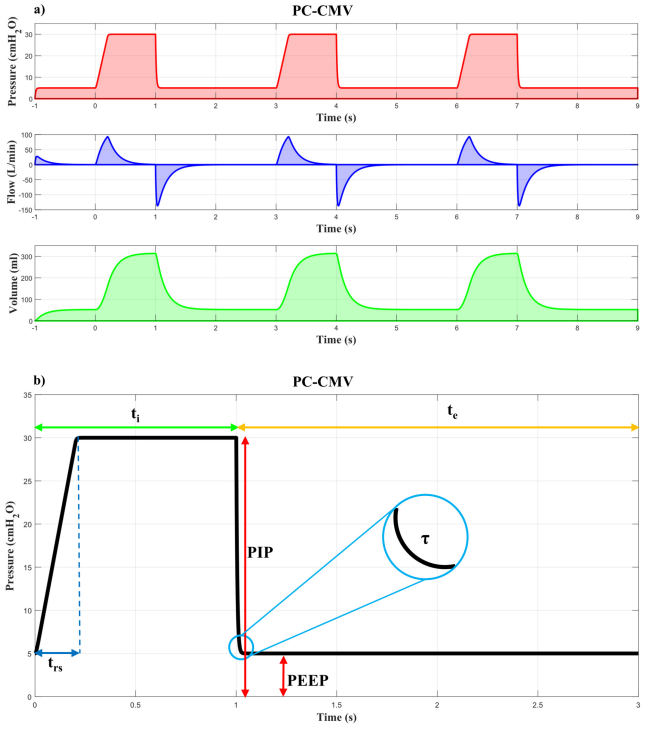

Fig. 1. Waveforms of Pressure (top) / Flow (middle) / Volume (bottom) vs Time. a) PC-CMV and b) parameters. c) VC-CMV. d) FC-CMV

Therefore, this paper presents the design and simulation of an algorithm for mandatory mechanical ventilation by volume controlled mode, and especially, pressure controlled mode (Fig. 1). The mechanical transfer function of the algorithm is based on the multi-compartmental linear mathematical model of the respiratory system, which consider their physiological resistances and compliances. Finally, the characterization of the algorithm is performed by varying the input parameters of the mechanical ventilator and ranging the values of resistance and lung compliance of patients with respiratory conditions.

*This project was funded by the *BBVA Foundation*.

[1] Biomedical Engineering Program PUCP-UPCH, Pontificia Universidad Catolica del Peru, Lima, Perú.
[2] Biomedical Engineering Program PUCP-UPCH, Universidad Peruana Cayetano Heredia, Lima, Perú.
[3] Department of Engineering, Pontificia Universidad Catolica del Peru, Lima, Perú.
**Corresponding author: victor.ticllacuri@pucp.edu.pe

II. Mathematical Model

The linear mathematical model used to mechanically emulate the respiratory system is based on the one proposed by [3]. This multi-compartment model is represented by the electrical circuit shown in figure 2, where the parameters are described in the table I, and mathematically denoted by differential equation 1. In addition, the Laplace transform allows to derive a relationship between pressure-flow and pressure-volume; both expressed in equation 2.

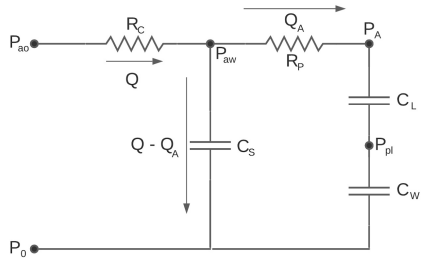

Fig. 2. Electrical circuit representation of multi-compartment linear model for respiratory mechanics.

TABLE I. Parameters of linear model for respiratory mechanics.

Parameter	Description	Units
R_C	Mechanical resistance of fluids of the central airways.	$\frac{cmH_2O}{L/s}$
R_P	Mechanical resistance of fluids of the peripheral airways.	
C_L	Compliance of the lung.	$\frac{L}{cmH_2O}$
C_S	Compliance of the alveoli.	
C_W	Compliance of the chest wall.	
C_T	$(1/C_L + 1/C_W + 1/C_S)^{-1}$	
P_{ao}	Pressure developed at the opening of the airways.	cmH_2O
P_{aw}	Pressure developed in the central airways.	
P_A	Pressure developed in the alveoli.	
P_{pl}	Pressure developed in the pleural space.	
P_0	Environmental pressure.	
Q	Volumetric flow of air entering to the respiratory system.	L/s
Q_A	Flow derived from the alveolus.	

III. Algorithm Design

The functional design of the algorithm was developed in MATLAB R2020a software (Mathworks Inc.) and takes into consideration the linear multi-compartment model (fig. 2 and eq. 1) to represent the respiratory system. Furthermore, their Laplace transforms denotations (eq. 2) are taken as the main transfer function of the algorithm in order to obtain the flow and volume from the inlet pressure.

Therefore, table II defines the general inputs and outputs of the algorithm based on the mechanical ventilation parameters.Finally, the algorithm also has inputs to set the simulation time (t_s), apply a rise slope (t_{rs}) and smooth the waves (τ) (fig. 1.b).

First, we generate the time signal with the vectorization of the simulation time (t_s) [0, t_s] with 1ms as sample period. Then, a vector [-1, 0[is added for PEEP regularisation,

TABLE II. Inputs and Outputs parameters of the simulation algorithm

	Parameter	Description	Units
Inputs (scalar)	$PEEP$	Positive End Expiratory Pressure	cmH_2O
	PIP	Peak Inspiratory Pressure	
	RF	Respiratory Frequency	RPM
	I/E	Inspiratory-Expiratory Ratio	(Ratio)
	FiO_2	Fraction of Inspired Oxigen	%
Outputs (vectorial)	Time	Time signal (vectorised)	s
	Pressure	Pressure signal (generated)	cmH_2O
	Flow	Flow signal (simulated)	L/s
	Volume	Volumen signal (simulated)	L

thus obtaining a time signal [-1,t_s]. Second, to generate the pressure signal, the time vector enters into a square wave generator with frequency = RF, duty cycle = $100\%\frac{(t_i)}{(t_i+t_e)}$ and amplitude = $PIP - PEEP$; where t_i and t_e are the inspiratory and expiratory times respectively (fig. 1.b). Then, t_{rs} defines a ramp/slope of 0.2s to generate the trapezoidal waveform, to which the PEEP is finally added as positive offset and smoothed with a first-order transfer function having τ = 5ms (fig. 1.b). Third, the pressure signal enters the principal transfer function (eq. 2) to generate the flow and volume signal, respectively.

IV. Methods

In order to characterise the algorithm with regard to variations in the mechanical ventilator parameters, a minimum and maximum respiratory frequency (RF) of 10 and 40 respirations per minute (RPM) respectively, as well as a minimum and maximum I/E ratio of 1/1 and 1/5 respectively, are taken.

On the other hand, to characterise the algorithm under multiple patient parameter scenarios, central airway resistance (R_C) is varied from 0.5 to 1.5 $cmH_2O/L/s$; as well as lung compliance (C_L) is varied from 0.1 to 0.3 L/cmH_2O.

Finally, for characterisation of the algorithm in a hypothetical COVID-19 patient case, an increased R_P is set to 1.5 $cmH_2O/L/s$ and a decreased C_L to 0.1 L/cmH_2O, while using the standard ventilation parameters.

V. Results

The comparison point is taken as the pressure-flow-volume (P-F-V) graph of the standard case (fig. 1.a): $RF = 20$, $IE = 1/2$ and $R_C = 1$, $C_L = 0.2$.

A. Regarding ventilator parameters

Figures 3.a and 3.b show the P-F-V graphics at an RF of 10 and 40 RPM respectively. At 10 RPM both flow and volume stabilise during t_i and t_e; however, at 40 RPM they do not as the pressure changes before. Similarly, figures 3.c and 3.d show the P-F-V graphics at an I/E ratio of 1/1 and 1/5 respectively. Analogous to 10 and 40 RPM respectively, at a 1/1 ratio both flow and volume stabilise for t_i and t_e; however, at a 1/5 ratio they do not as the pressure changes faster. Therefore, note the similarities in wave-forms between 10 RPM and a 1/1 ratio, as well as between 40 RPM and a 1/5 ratio.

$$\frac{d^2P_{ao}}{dt^2} + \frac{1}{R_P C_T}\frac{dP_{ao}}{dt} = R_C\frac{d^2Q}{dt^2} + (\frac{1}{C_S} + \frac{R_C}{R_P C_T})\frac{dQ}{dt} + \frac{1}{R_P C_S}(\frac{1}{C_L} + \frac{1}{C_W})Q \tag{1}$$

$$\frac{F(s)}{P(s)} = \frac{s^2 + (\frac{1}{R_P C_T})s}{R_C s^2 + \left(\frac{1}{C_S} + \frac{R_C}{R_P + C_T}\right)s + (\frac{1}{R_P C_S})\left(\frac{1}{C_L} + \frac{1}{C_W}\right)} \quad \xrightarrow{integration} \quad \frac{V(s)}{P(s)} = (\frac{1}{s})\frac{F(s)}{P(s)} \tag{2}$$

B. Regarding patient parameters

Figures 4.a and 4.b show the P-F-V and PV loop plots of the superimposed variations of C_L, respectively. Then, the higher C_L, the higher the maximum volume, but also the longer settle time. Additionally, in PV loop, the maximum/minimum/tidal volume increase exponentially to the increase of C_L.

Moreover, figures 4.c and 4.d show the P-F-V and PF loop plots of the superimposed variations of R_P, respectively. Then, the higher R_P, the lower the absolute maximum flow and the slightly longer settle time. Additionally, in PF loop, positive/negative/maximum flow decrease exponentially to the increase of R_P. Note the waveform of the middle, both in the pressure, flow and volume graphics as well as in the PV and PF loop, corresponds to the standard case.

C. Regarding COVID-19

Finally, figures 5.a and 5.b shows the P-F-V and PF-PV loops of the comparison between the parameters of a healthy patient and one infected with COVID-19, respectively. In the COVID-19 case, note the peak flow decreases as well as the peak volume. Thus, the positive and negative peak flow decreases, as well as the tidal volume. These results, respond adequately with respect to the variations previously shown.

VI. Discussion

A. About ventilatory parameters

Peak flow rate, and hence peak volume, depends on PEEP, PIP and slope, as well as the patient's airway resistance and lung compliance. Thus, if the inspiratory time is long enough for the alveolar pressure to equilibrate to the set pressure, the inspiratory flow waveform returns to baseline (fig. 1.a) [4].

However, if the inspiratory time is not long enough for the alveolar pressure to reach the PIP, the inspiratory flow waveform does not return to baseline, thus producing a reduced peak volume, which is generated at 40 RPM and at a 1/5 ratio [4]. On the other hand, if inspiratory time continues after inspiratory flow has returned to the zero flow baseline, an inspiratory pause occurs, which is generated at 10 RPM and at a ratio of 1/1 [4].

B. About patient parameters

The resistance R_C can be expressed mathematically by the Hagen-Poiseuille equation $\Delta P = Q * R = Q * (8\eta l/\pi r^4)$ where η=viscosity, l=length and r=radius, assuming laminar flow [5]. Here, radius is the most important factor, as it can produce a significant change in airway resistance with only a small change, due to its fourth power. Thus, the smaller the radius, the greater the resistance and hence the higher the peak airway flow (by Bernoulli's principle), but with no significant variation in peak volume (by the conservation of mass principle).

Clinically, drastic variations in flow due to constriction (mainly) or dilatation of the airways imply severe changes in patients, so clinicians seek to regulate them rapidly [5]. These changes in airway radius can be caused by multiple pathologies, but primarily Asthma ($\uparrow R_P$), chronic bronchitis ($\uparrow R_P$) and Emphysema ($\downarrow R_P$).

On the other hand, C_L is the volume change in lungs for a given change in transpulmonary pressure. In this way, C_L is an indicator of the lung parenchyma's physiological characteristics, as it depends on specific factors such as the elastic properties (collagen and elastin fibres mesh) and the surface tension of alveolar lining (secreted surfactant) [6].

Therefore, for this study, variation in C_L represents changes in the mechanical characteristics of the lung parenchyma and its relationship to the pleural layers and thorax. Clinically, variations in lung compliance are the product of multiple pathologies, especially emphysema ($\uparrow C_L$), Pulmonary fibrosis ($\downarrow C_L$) and atelectasis/Acute Respiratory Distress Syndrome (ARDS) ($\downarrow C_L$).

C. About COVID-19

The SARS-CoV-2 virus generates multiple physiological responses in the patient, most notably for this study, airway constriction, alveolar collapse and fibrosis in the lung parenchyma. As seen in subsection VI-B, these physiological responses can be interpreted as mechanical variables of interest for ventilation.

Constriction of the main airways leads to an increase in R_P beacuse of bronchospasms, airway inflammation, and increased mucus, significantly decreasing the airway lumen; similar to asthma and chronic bronchitis. Likewise, fibrosis and loss of functional lung parenchyma leads to reduced C_L beacuse of the alveoili colapse, in responses; similar to pulmonary fibrosis or ARDS.

D. About mathematical model

Finally, this mathematical model allows us to predict the behaviour of both the maximum, minimum and tidal volume with respect to C_L (fig. 6); as well as the positive, negative and maximum flow with respect to R_C (fig. 7). These curves are properly fitted ($R^2 = 0.9996$) to a second-degree exponential equation described by the eq. 3, whose coefficients (with 95% confidence bounds) are shown in table III. This modelling would allow both lung compliance and

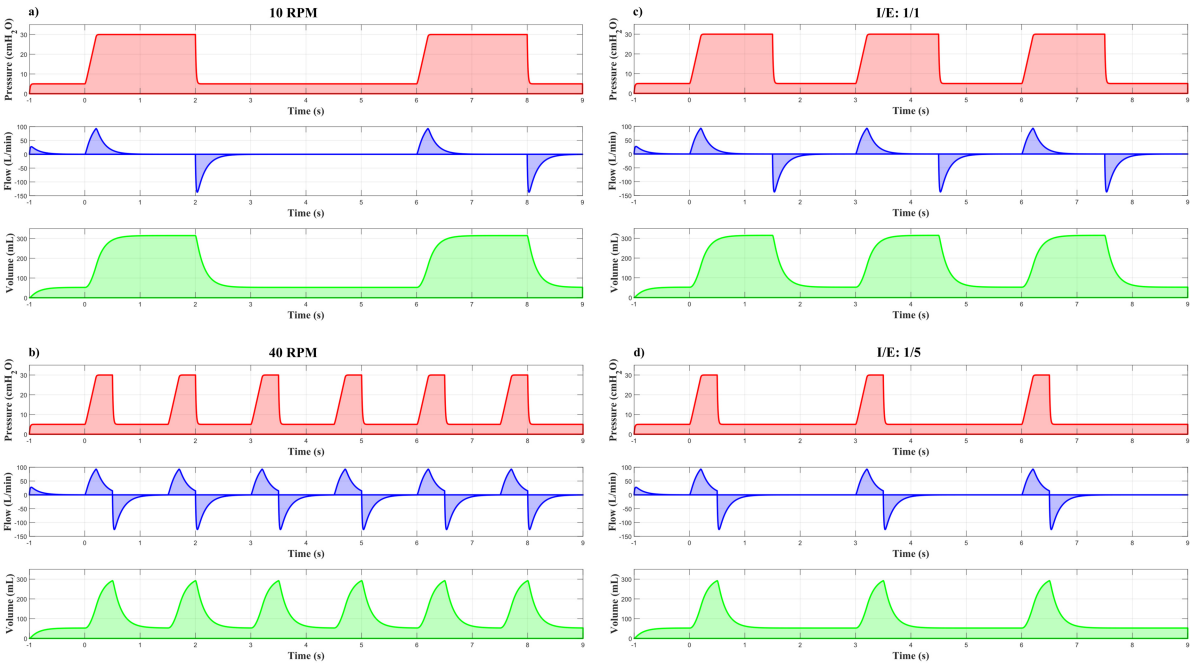

Fig. 3. PC-CMV waveforms of Pressure/Flow/Volume vs Time under variations of RF and I/E. a) RF: 10 RPM. b) RF: 40 RPM. c) I/E: 1/1. d) I/E: 1/5

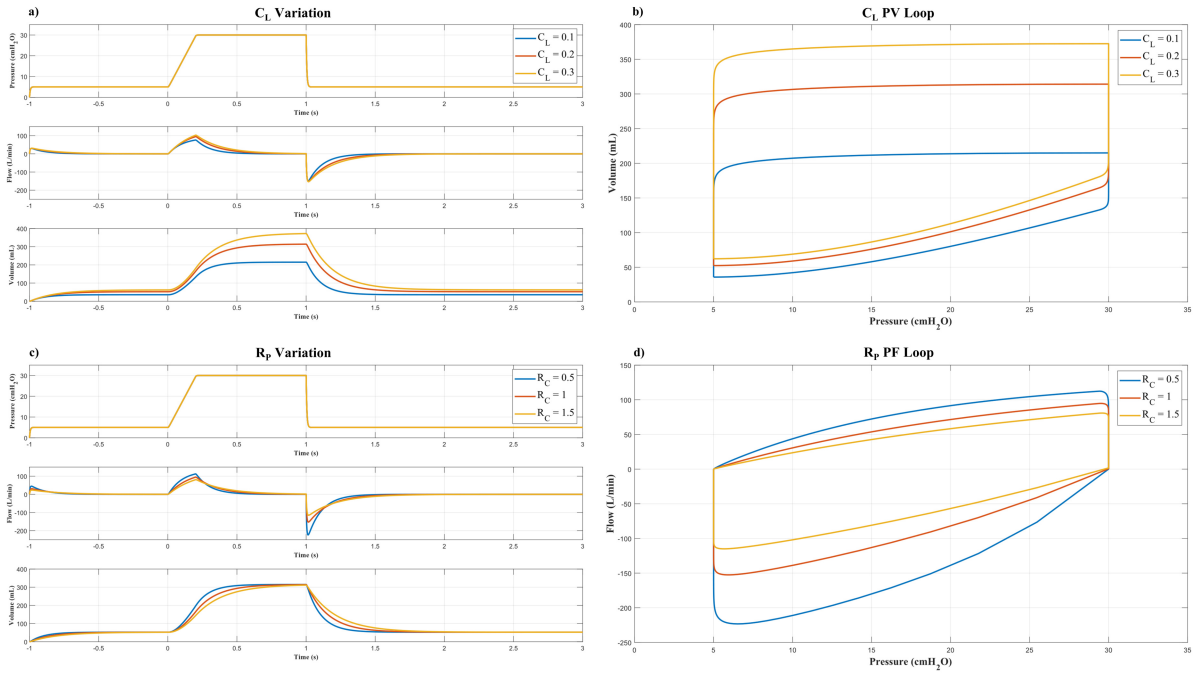

Fig. 4. PC-CMV waveforms of Pressure/Flow/Volume vs Time and PV and PF loops under variations of C_L and R_P. a) P-F-V waveforms and b) PV Loop with variation of C_L. c) P-F-V waveforms and d) PF Loop with variation of R_C.

airway resistance to be known directly from the volume and flow variables of a mechanical ventilator. This implies a better understanding of the pulmonary status of patients.

$$y = \alpha e^{\mu_1 x} + \beta e^{\mu_2 x} \tag{3}$$

VII. Conclusion

The presented algorithm demonstrates the effectiveness of computationally simulating the variation of the parameters of lung compliance and airway resistance, as well as the pressure, volume and flow waveform responses. However, the experimental implementation on a high-end mechanical ventilator is necessary in order to contrast with experimental results and parameters.

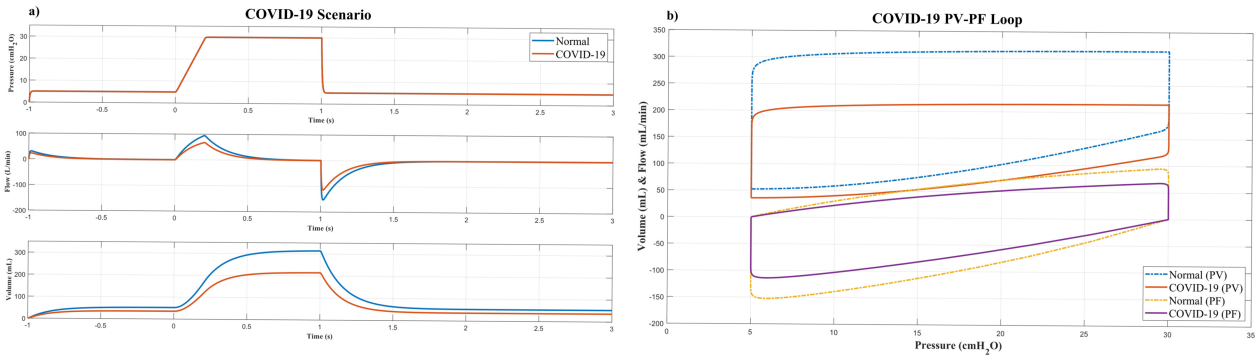

Fig. 5. Comparation of a) PC-CMV waveforms of Pressure/Flow/Volume vs Time. b) PV and PF loops under emulated normal and COVID-19 conditions

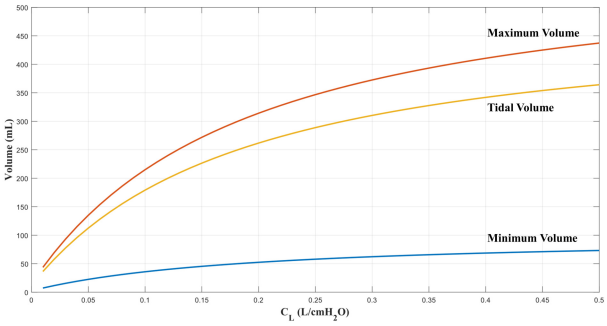

Fig. 6. Evolution of minimum/maximum/tidal Volume vs C_L

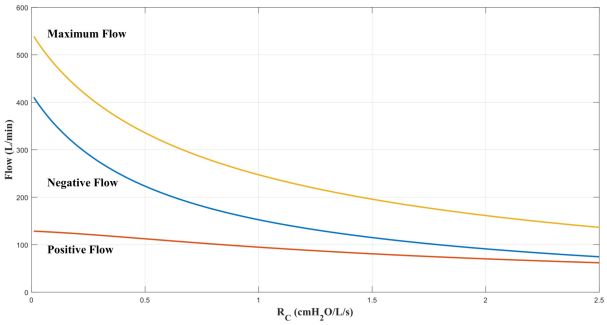

Fig. 7. Evolution of positive/negative/maximum Flow vs C_L

TABLE III. Curve fitting coefficients

		Coefficients			
		α	β	μ_1	μ_2
Volume ($x = C_L$)	Min	68.53	-63.66	0.2148	-6.03
	Max	409.5	-380.5	0.2135	-6.079
	Tidal	340.9	-316.8	0.2132	-6.089
Flow ($x = R_C$)	Max +	109.2	23.01	-0.4327	0.03476
	Max -	228.3	178.4	-2.251	-0.3447
	Abs	269.8	261.7	-1.819	-0.2634

Finally, this algorithm could provide a more personalised treatment for adult patients with respiratory conditions, including COVID-19, by providing insight into their respiratory parameters. In addition, it could be used for education on the functioning, modeling and simulation of the respiratory system, in universities and educational programs such as the joint program Biomedical Engineering PUCP-UPCH.

ACKNOWLEDGMENTS

This work has been funded by the *Perú BBVA Foundation* (PI0726-PUCP-5) and supported by the *Laboratorio de Investigación en Biomecánica y Robótica Aplicada* (LIBRA). The authors would like to thank Dante Elias and Victoria Abarca for their advice on project management.

REFERENCES

[1] J. Chang, A. Acosta, J. Benavides-Aspiazu, *et al.*, "Masi: A mechanical ventilator based on a manual resuscitator with telemedicine capabilities for patients with ards during the covid-19 crisis," *Hardwarex*, vol. 9, e00187, 2021.

[2] S. Morales, S. Palomino, R. Terreros, *et al.*, "Pressure and volume control of a non-invasive mechanical ventilator: A pi and lqr approach," pp. 67–71, 2021. DOI: 10.1109/ICCMA54375.2021.9646186.

[3] M. Khoo, *Physiological Control Systems*. John Wiley Sons, Inc., Jul. 2018, ISBN: 9781119058786. DOI: 10.1002/9781119058786.

[4] L. Ashworth, Y. Norisue, M. Koster, J. Anderson, J. Takada, and H. Ebisu, "Clinical management of pressure control ventilation: An algorithmic method of patient ventilatory management to address "forgotten but important variables"," *Journal of Critical Care*, vol. 43, pp. 169–182, Feb. 2018, ISSN: 0883-9441. DOI: 10.1016/J.JCRC.2017.08.046.

[5] J. H. Bates, "Systems physiology of the airways in health and obstructive pulmonary disease," *Wiley interdisciplinary reviews. Systems biology and medicine*, vol. 8, pp. 423–437, 5 Sep. 2016, ISSN: 1939-005X. DOI: 10.1002/WSBM.1347.

[6] D. Papandrinopoulou, V. Tzouda, and G. Tsoukalas, "Lung compliance and chronic obstructive pulmonary disease," *Pulmonary medicine*, vol. 2012, 2012, ISSN: 2090-1844. DOI: 10.1155/2012/542769.